Chaos, Solitons and Fractals 159 (2022) 112035

Contents lists available at ScienceDirect

Chaos, Solitons and Fractals

Nonlinear Science, and Nonequilibrium and Complex Phenomena

journal homepage: www.elsevier.com/locate/chaos

Controlling COVID-19 transmission with isolation of influential nodes

Sarkhosh Seddighi Chaharborj [a,b], Khondoker Nazmoon Nabi [c,*], Koo Lee Feng [d], Shahriar Seddighi Chaharborj [e], Pei See Phang [f,g]

[a] School of Mathematics and Statistics, Carleton University, Ottawa K1S 5B6, Canada
[b] Department of Mathematical Sciences, Universiti Teknologi Malaysia, Johor Bahru 81310, Malaysia
[c] Department of Mathematics, Bangladesh University of Engineering and Technology (BUET), Dhaka, Bangladesh
[d] Department of Science and Technology, University Putra Malaysia, Campus Bintulu, 97000 Bintulu, Sarawak, Malaysia
[e] Department of Mathematics, Faculty of Science, Tabriz Branch, Islamic Azad University, Tabriz, Iran
[f] Department of Mathematics, Faculty of Science, Universiti Putra Malaysia, 43400, UPM, Malaysia
[g] Brilliant Student Care 838, Jurong West Street 81, 640838, Singapore

ARTICLE INFO

Article history:
Received 19 July 2021
Received in revised form 20 December 2021
Accepted 22 March 2022
Available online 5 April 2022

Keywords:
Complex network
TOPSIS method
Vital spreaders identification
Epidemic model
Transmission probability
Node-ranking

ABSTRACT

To understand the transmission dynamics of any infectious disease outbreak, identification of influential nodes plays a crucial role in a complex network. In most infectious disease outbreaks, activities of some key nodes can trigger rapid disease transmission in the population. Identification and immediate isolation of those influential nodes can impede the disease transmission effectively. In this paper, the technique for order of preference by similarity to ideal solution (TOPSIS) method with a novel formula has been proposed to detect the influential and top ranked nodes in a complex social network, which involves analyzing and studying of structural organization of a network. In the proposed TOPSIS method, several centrality measures have been used as multi-attributes of a complex social network. A new formula has been designed for calculating the transmission probability of an epidemic disease to identify the impact of isolating influential nodes. To verify the robustness of the proposed method, we present a comprehensive comparison with five node-ranking methods, which are being used currently for assessing the importance of nodes. The key nodes can be considered as a person, community, cluster or a particular area. The Susceptible-infected-recovered (SIR) epidemic model is exploited in two real networks to examine the spreading ability of the nodes, and the results illustrate the effectiveness of the proposed method. Our findings have unearthed that quarantine or isolation of influential nodes following proper health protocols can play a pivotal role in curbing the transmission rate of COVID-19.

1. Introduction

Spreading process is a natural phenomenon and it is often found in biological, electrical, social, chemical, and many other fields. Complex networks have been used comprehensively in determining the most effective nodes and spreading ability-based ranking [1,2]. In comparison to other nodes, influential nodes play an important role in complex networks in many applications like viral marketing, rumour spreading, disease outbreak and so on. However, selecting a set of influential nodes may demand taking the mutual influence into account between the nodes instead of simply selecting nodes with substantial influence. In addition, it is seriously challenging to select the initial node-set for maximizing spreading scale after the propagation process. To analyze and control the information dissemination process, complex networks require identifying influential network spreads [3–5]. Influential spreaders are the critical nodes running as a controller or a maximizer of a spread process in a complex network. For instance, an epidemiological network manages the virus propagation by controlling such influential nodes behavior, which expands information propagation in a social network using them as a maximizer [6]. In the literature, multiple indexing methods have been proposed to determine the influential network spreaders [7–9]. The real world consists of many complex networks, including social networks, biological networks, research networks, and transport networks. Real-world complex networks are unconstrained and often can be categorized as unweighted and undirected. Identifying and controlling the information propagation process in such networks significantly contributes to decision-making activities. It has many functions, such as market advertising, rumor control, disease control, and innovation propagation. As influencers are critical actors for information spread to help the decision-making process, it is necessary to identify influencers in complex networks [10–15].

* Corresponding author.
E-mail addresses: sseddighi2014@yahoo.com.my (S.S. Chaharborj), knabi@g.harvard.edu (K.N. Nabi).

https://doi.org/10.1016/j.chaos.2022.112035
0960-0779/

In recent times, analysis of complex networks has been widely used and developed due to its high correlation with various research issues. Recently, various relevant studies have been carried out to study the significant properties of the complex networks and how they become useful in modeling evidence theory and different decision-making scenarios [16–20]. Ye et al. [21] studied group behavior adaptability and welfare dynamics adaptability in multi-agent dynamics by adopting co-evolution of game dynamics and network structure. Ranking the influential nodes in a complex network and knowledge-based system has been really popular in recent times, as this concept is really insightful in various fields. Liu et al. [22] proposed a generalized mechanical model incorporating both local and global information to identify the influential nodes in a complex network. In this work, ten real networks have been used to verify the effectiveness of the proposed method. To address the limitations of several centrality measures, Wen et al. [23] proposed a multi-local dimension (MLD) based on fractal property to identify the vital spreaders in complex networks. To show the effectiveness and reasonableness of the proposed method, some real-world and theoretical complex networks are exploited in the study. There are numerous real-life applications of complex networks in evidence theory. To visualize the relationship between individuals, Zhao and Deng [24] proposed a complex network model of evidence theory based on the similarity of evidence. In a recent work [25], structural similarity of nodes has been considered and original transition matrix has been replaced by similarity matrix to incorporate the fact that the transition probability between nodes and their neighbors is not same. Based on node ranking methods, Yu et al. [26] introduced a novel re-ranking algorithm through information spread function to determine a set of influential nodes for complex networks. Yang et al. [27] studied how to identify influential spreaders in complex networks based on node-local centrality and network embedding. Several approaches have been proposed from different perspectives to identify critical nodes in complex networks. Among these, the gravity model can effectively find significant nodes based on local and path information. In this regard, Li et al. [28] used a generalized gravity model for identifying influential spreaders in complex networks. Namtirtha et al. [6] provided the best method of identifying influential spreaders based on network global structural properties. Gupta and Mishra [29] studied information dissemination in complex networks and identified a set of top-N influential nodes using network structure.

In an epidemiological network, virus propagation can be controlled by analysing the behavior of influential nodes. From any topological position, spreading process can be controlled by calculating each node's spreading capability. As several mass vaccination programs of COVID-19 are going on in different countries, several virulent variants of COVID-19 have started posing threats of new surges of cases. From the beginning of COVID-19 pandemic, numerous mathematical modeling approaches have contributed a lot in terms of designing resilient public health policies to control the disease transmission [30–33,42]. However, effective identification of influential spreaders is still a puzzle to be solved. In this paper, the technique for order of preference by similarity to ideal solution (TOPSIS) method with a novel formula has been proposed to identify the influential spreaders efficiently in a complex social network, which involves analyzing and studying of structural organization of a network. Though numerous node-ranking methods are available in the literature, experimental results highlight that our proposed method outperforms all the contemporary methodologies over a large variety of network connectivity structures. Our proposed method is competitive with more sophisticated approaches that are computationally costly. It has been found in our experimental results that our proposed method can identify the most influential spreaders efficiently from complex networks. As the real disease transmission rate varies from network to network, infection probability is an insightful parameter to understand the real disease spreading scenario. Even though it is difficult to estimate real infection rate of a network, we have calculated disease spread probability pertinent to network epidemic threshold. Two real COVID-19 networks have been used to validate the robustness of the proposed method in identifying and ranking influential nodes. Eventually, a comprehensive comparison with the contemporary methods is presented to illustrate the effectiveness of the proposed method.

2. Materials and methods

Effective and influential identification of influential people or organizations can be helpful in controlling COVID-19 spread. In this section, several methods are presented to identify important nodes in random networks. Identifying influential propagators in the social or complex networks is a major challenge. To address this problem, several centrality measures such as eigenvector centrality (EC), degree centrality (DC), betweenness centrality (BC), and closeness centrality (CC) are proposed here. In the following, TOPSIS along with new modified weights are proposed to identify important and influential nodes.

2.1. Node ranking using centrality measures

In this section, centrality measures such as DC [14], CC [15], BC [16], and EC [12] are proposed to identify the influential and important nodes within a complex or social network. Inverse sum of the shortest distances from a central node to all other nodes denotes closeness centrality. Therefore, the higher the score of closeness centrality is, the closer the node to others. Betweenness measures number of the shortest paths through a node. Eigenvector centrality, which is another method to detect important and influential nodes, was first presented by Bonacich [17]. In the eigenvector centrality method, importance and influence of a node is based on the number of neighbors and their quality. The DC, CC, BC, and EC methods are defined as follows:

a. Degree centrality

The degree centrality (DC) of node i, denoted as $C_D(i)$, is defined as:

$$C_D(i) = \sum_{j=1}^{N} x_{ij} \tag{1}$$

where, N is the total number of nodes, i is the focal node, j represents all other nodes, and x_{ij} represents the connection between node i and node j. If node i is connected to node j, the value of x_{ij} is 1 and otherwise, it is 0. By minimizing the number of mediator nodes, the shortest path is found in a binary network, and the minimum number of ties grafting the two nodes either directly or indirectly define its length [14]. The binary shortest distance is defined as follows [18],

$$d(i,j) = \min_{h} \left(x_{ih} + \ldots + x_{hj}\right) \tag{2}$$

Here, the number of mediator nodes on the path between nodes i and j is defined by h.

b. Closeness centrality method

The closeness centrality $C_C(i)$ for node i is defined as follows:

$$C_C(i) = \left(\sum_{j=1}^{N} d_{ij}\right)^{-1}, \tag{3}$$

Where, d_{ij} is the distance between node i and node j.

c. Betweenness centrality method

The betweenness centrality $C_B(i)$ for node i is defined as:

$$C_B(i) = \frac{N(N-1)}{2}\left(\sum_{k \neq i \neq l}^{N} \frac{p_{kl}(i)}{p_{kl}}\right)^{-1}, \tag{4}$$

With the following definitions for parameters p_{kl}, $p_{kl}(i)$ and $\frac{N(N-1)}{2}$
p_{kl}: number of binary shortest paths between node k and node l,
$p_{kl}(i)$: number of paths that go through node i.
$\frac{N(N-1)}{2}$: used to normalize the betweenness centrality value.

d. Eigenvector centrality method

If A be an $n \times n$ similarity matrix, then the eigenvector centrality x_i of node i is defined as follows:

$$Ax = \lambda x, \;\; x_i = \frac{1}{\lambda}\sum_{j=1}^{n} a_{ij}x_j, i = 1, \ldots, n \tag{5}$$

where, x_i is the ith entry in the normalized eigenvector belonging to the largest eigenvalue of matrix A, a_{ij} is array of similarity matrix A, λ is the largest eigenvalue and n is the number of vertices.

2.2. Weighted TOPSIS method

The TOPSIS method [19] was developed by Hwang and Yoon in 1981 [20]. It is a ranking conception and application method in a social or complex network. The standard TOPSIS method is for the selection of a solution that simultaneously has the farthest distance from the negative ideal solution and shortest distance from the positive ideal solution. Maximizing the benefit criteria and minimizing the cost criteria is positive ideal solution, whereas minimizing the benefit criteria and maximizing the cost criteria is negative ideal solution.

Definition 1.2. Suppose $\mathrm{D} = (\mathrm{x_{mn}})$ be a decision matrix, which consists of criteria and alternatives. The decision matrix $\mathrm{R} = (\mathrm{r_{ij}})$ can be normalized as follows,

$$\mathrm{r_{ij}} = \mathrm{x_{ij}} \times \left(\sqrt{\sum_{\mathrm{k=1}}^{\mathrm{N}} (\mathrm{x_{ik}})^2}\right)^{-1}, \mathrm{i} = 1, \ldots, \mathrm{N}; \mathrm{j} = 1, \ldots, \mathrm{m}. \tag{6}$$

Weighted decision matrix $A = (v_{mn})$ can be derived by multiplying the related weights in the columns of the normalized decision matrix as follows,

$$v_{ij} = w_j \times r_{ij}, i = 1, \ldots, N; j = 1, \ldots, m. \tag{7}$$

Where w_j is the weight for j criterion. In this paper, the new weights are proposed as follows:

$$w_j = \frac{\sum_{i=1}^{N} r_{ij}}{\sum_{i=1}^{N}\sum_{j=1}^{m} r_{ij}}, i = 1, \ldots, N; j = 1, \ldots, m. \tag{8}$$

The positive-ideal solution and the negative-ideal solution are defined as follows:

$$A^+ = \{v_1^+, \ldots, v_n^+\} = \left\{\left[\max_i (v_{ij}) | j \in K_b\right] \times \left[\min_i (v_{ij}) | j \in K_c\right]\right\} \tag{9}$$

$$A^- = \{v_1^-, \ldots, v_n^-\} = \left\{\left[\min_i (v_{ij}) | j \in K_b\right] \times \left[\max_i (v_{ij}) | j \in K_c\right]\right\} \tag{10}$$

Where, K_b and K_c are the set of benefit criteria and the set of cost criteria, respectively. From the solutions A^+ and A^-, we have,

$$S_i^+ = \sqrt{\sum_{j=1}^{m} \left(v_j^+ - v_{ij}\right)^2}, i = 1, \ldots, N; j = 1, \ldots, m \tag{11}$$

$$S_i^- = \sqrt{\sum_{j=1}^{m} \left(v_j^- - v_{ij}\right)^2}, i = 1, \ldots, N; j = 1, \ldots, m \tag{12}$$

Solutions S_i^+ and S_i^- are the separation measures based on Euclidean distance. Using the positive ideal and negative ideal solutions S_i^+ and S_i^-, the relative closeness can be calculated as,

$$C_i = \frac{S_i^-}{S_i^- + S_i^+}, i = 1, \ldots, N. \tag{13}$$

All nodes are ranked based on the relative closeness to the ideal solution. It means that the influential and higher priority nodes have higher C_i.

2.3. Analysis of time complexity

The time complexity is involved in calculating the weighted decision matrix. The complexity of this step is based on each iteration. One matrix multiplication with a vector is needed where time complexity is $O(n^2)$, where n is the length of the vector. However, in case of sparse matrix with on average m non-zero elemets on every row, the matrix multiplication with a vector can instead be done in $O(mn)$ time.

2.4. Testing of the proposed method

In this Section, four graph networks as showed in the Figs. 1–4, from previous published papers [1,34–36] are presented to illustrate the application of centrality measures and proposed method based on relative closeness to the ideal solution. First network containing 12 nodes and 13 edges is presented from reference [34]. Fig. 1 shows the proposed network with four top ranking nodes highlighted with red color.

Based on the connected and unconnected nodes for the first graph as showed in the Fig. 1, the adjacency matrix for this graph is as follows,

$$adj = \text{Adjacency Matrix} = \begin{bmatrix} 0&0&0&1&0&1&0&0&0&0&0&0\\ 0&0&0&1&0&0&0&0&0&0&0&0\\ 0&0&0&1&0&0&0&0&0&0&0&0\\ 1&1&1&0&1&0&0&0&0&0&0&0\\ 0&0&0&1&0&1&1&0&0&0&0&0\\ 1&0&0&0&1&0&1&0&0&0&0&0\\ 0&0&0&0&1&1&0&1&0&0&0&0\\ 0&0&0&0&0&0&1&0&1&1&1&1\\ 0&0&0&0&0&0&0&1&0&0&0&0\\ 0&0&0&0&0&0&0&1&0&0&0&0\\ 0&0&0&0&0&0&0&1&0&0&0&0 \end{bmatrix}_{12\times 12}$$

Therefore, the decision matrix $D = (x_{ij})$ for the graph 1 be obtained as follows,

Three centrality measures of DC, BC, and EC as shown in Table 1 are employed to derive the decision matrix. Eq. (6) can be used to normalize the decision matrix, and then the normalized decision matrix $R = (r_{ij})$ is derived as follows,

$$r_{52} = \frac{x_{52}}{\sqrt{\sum_{k=1}^{N} (x_{5k})^2}} = \frac{\mathbf{13}}{\sqrt{68^2 + 60^2 + \ldots + 0^2 + 0^2}} = 0.2214 \simeq \mathbf{0.22},$$

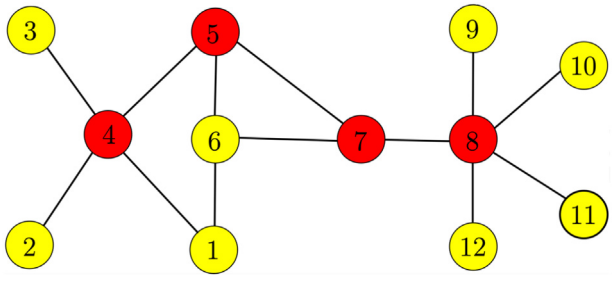

Fig. 1. A network containing 12 nodes and 13 edges [34]. Four top ranking nodes highlighted with red color.

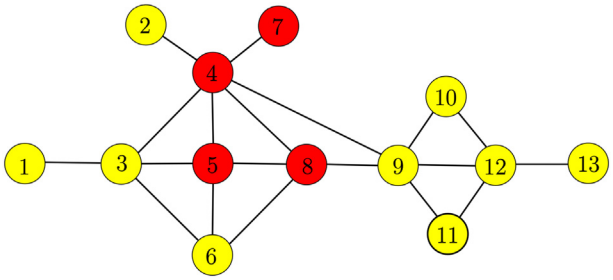

Fig. 2. A network containing 13 nodes and 19 edges [35]. Four top ranking nodes highlighted with red color.

$$R=\begin{bmatrix} 0.23 & 0.11 & 0.11 & 0.45 & 0.34 & 0.34 & 0.34 & 0.57 & 0.11 & 0.11 & 0.11 & 0.11 \\ 0.27 & 0.36 & 0.36 & 0.26 & \mathbf{0.22} & 0.24 & 0.20 & 0.22 & 0.31 & 0.31 & 0.31 & 0.31 \\ 0.028 & 0.00 & 0.00 & 0.36 & 0.36 & 0.12 & 0.56 & 0.63 & 0.00 & 0.00 & 0.00 & 0.00 \end{bmatrix}^{T}$$

Here, T is transpose of matrix R. Eq. (8) is used to obtain weighted decision matrix $A=(v_{mn})$ as,

$$\begin{aligned} w_1 &= \frac{\sum_{k=1}^{12} r_{k1}}{\sum_{j=1}^{3}\sum_{k=1}^{12} r_{kj}} = \frac{r_{11}+\ldots+r_{121}}{(r_{11}+r_{12}+r_{13})+\ldots+(r_{121}+r_{122}+r_{123})} \\ &= \frac{0.23+0.11+\ldots+0.11}{(0.23+0.27+0.028)+\ldots+(0.11+0.31+0.00)} = \frac{2.9439}{8.4274} \\ &= \mathbf{0.3493}, \end{aligned}$$

$$w=\{\mathbf{0.3493}, 0.4044, 0.2462\},\ a_{25}=0.4044\times 0.2214=0.0896\simeq \mathbf{0.089},$$

$$A=\begin{bmatrix} 0.079 & 0.039 & 0.039 & 0.158 & 0.119 & 0.119 & 0.119 & 0.119 & 0.198 & 0.039 & 0.039 & 0.039 \\ 0.113 & 0.144 & 0.144 & 0.105 & 0.089 & 0.097 & 0.082 & 0.089 & 0.128 & 0.128 & 0.128 & 0.128 \\ 0.007 & 0.000 & 0.000 & 0.089 & 0.089 & 0.029 & 0.138 & 0.156 & 0.000 & 0.000 & 0.000 & 0.000 \end{bmatrix}^{T}$$

The new weights shown in the Eq. (8) were used to obtain the weighted decision matrix. The positive ideal solution A^+ and the negative ideal solution A^- are derived using Eqs. (9) and (10),

$$\begin{aligned} &\left\{\max_i (v_{ij}) | j\in K_b\right\} \\ &= max \\ &\{0.0791, 0.0396, 0.0396, 0.1582, 0.1187, 0.1187, 0.1187, 0.1978, 0.0396, 0.0396, 0.0396, 0.0396\} \\ &= \mathbf{0.1978}. \end{aligned}$$

$$\begin{aligned} &\left\{\min_i (v_{ij}) | j\in K_c\right\} \\ &= min \\ &\{0.0791, 0.0396, 0.0396, 0.1582, 0.1187, 0.1187, 0.1187, 0.1978, 0.0396, 0.0396, 0.0396, 0.0396\} \\ &= \mathbf{0.0396}. \end{aligned}$$

$$A^+=\{\mathbf{0.1978}, 0.1441, 0.1565\};\ A^-=\{\mathbf{0.0396}, 0.0818, 0.0000.\}$$

The separation measures S_i^+ and S_i^- are calculated using Eqs. (11) and (12), respectively as follows,

$$\begin{aligned} S_5^+ &= \sqrt{\sum_{j=1}^{3}\left(v_j^+ - v_{7j}\right)^2} \\ &= \sqrt{(0.1978-0.1187)^2+(0.1441-0.0896)^2+(0.1565-0.0898)^2} \\ &= \sqrt{0.0063+0.0030+0.0045} = \sqrt{0.0137} = \mathbf{0.1170}, \end{aligned}$$

$$\begin{aligned} S_5^- &= \sqrt{\sum_{j=1}^{3}\left(v_j^- - v_{7j}\right)^2} \\ &= \sqrt{(0.0396-0.1189)^2+(0.0818-0.0896)^2+(0.0000-0.0898)^2} \\ &= \sqrt{0.0063+0.0001+0.0081} = \sqrt{0.0144} = \mathbf{0.1199}, \end{aligned}$$

$$C_5=\frac{S_5^-}{S_5^- + S_5^+}=\frac{0.1199}{0.1199+0.1170}=\frac{0.1199}{0.2369}=\mathbf{0.5061}$$

The result of node ranking based on relative closeness to the ideal solution for the graph 1 (Fig. 1) is presented in the Table 2. According to Eq. (13), the values of C_i were calculated using the values of S_i^- and S_i^+. The largest value of C_i belongs to the node with the highest ranking in the network. As can be seen in the Table 2, $C_9 = \min_{i=1,\ldots,12}\{C_i\} = 0.1732$ and $C_7 = \max_{i=1,\ldots,12}\{C_i\} = 0.8034$. Therefore, node 8 is ranked first and node 9 is ranked last in the twelve ranked nodes of graph 1.

Node ranking based on relative closeness to the ideal solution for the graphs 2–4 (Figs. 2–4) are showed in the Table 3–5. According to Table 3, $C_2 = \min_{i=1,\ldots,13}\{C_i\} = 0.1693$ and $C_4 = \max_{i=1,\ldots,14}\{C_i\} = 0.7375$, then, node 4 is ranked first and node 2 is ranked last in the thirteen ranked nodes of graph 2. As can be seen in the Table 4, $C_5 = \min_{i=1,\ldots,23}\{C_i\} = 0.1593$ and $C_1 = \max_{i=1,\ldots,23}\{C_i\} = 0.8836$, therefore node 1 is ranked first and node 5 is ranked last in the twenty-three ranked nodes of graph 3. The results of Table 5 show, $C_{22} = \min_{i=1,\ldots,24}\{C_i\} = 0.0865$ and $C_1 = \max_{i=1,\ldots,24}\{C_i\} = 0.7479$. Therefore, node 1 is ranked first and node 22 is ranked last in the twenty-four ranked nodes of graph 4.

2.5. A new formula for disease spread probability in a complex network

In this Section, we study the disease spread probability in a complex network with quarantine of infected influential nodes. Supposing G as proposed graph, N as number of total nodes and E as number of

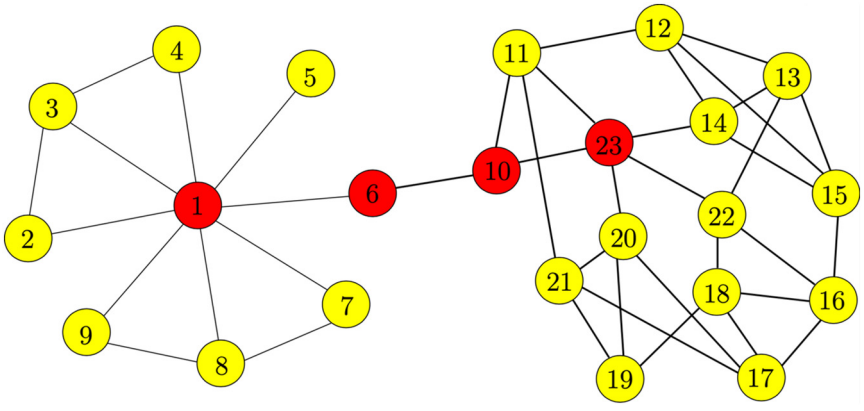

Fig. 3. An example network consisted of 23 nodes and 40 edges [1]. Although node 23 has lower degree than node 1, its influence may be even higher. Four top ranking nodes highlighted with red color.

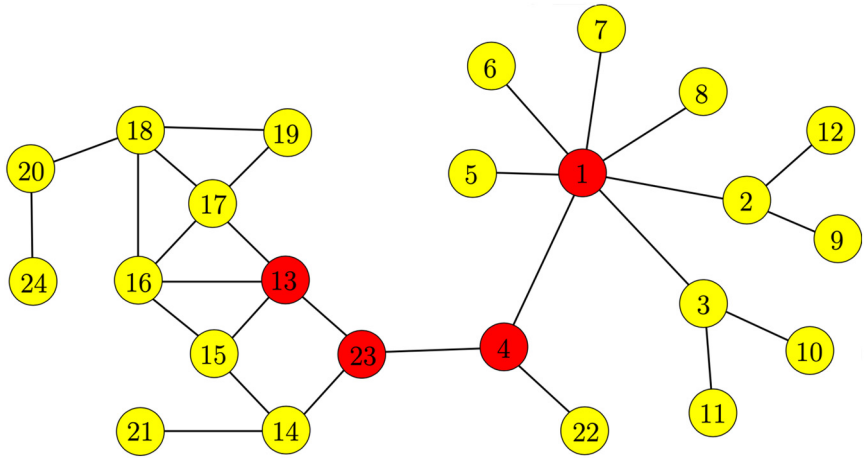

Fig. 4. An example network consisted of 24 nodes and 29 edges [36]. Although node 23 has lower degree than node 1, its influence may be even higher. Four top ranking nodes highlighted with red color.

influential nodes with top ranking, the pandemic spread probability $P(G_j)$ for the graph G_j can be defined as follows,

$$P(G_j) = \frac{N-j+1}{N} \times \frac{\sum_{k=1}^{N}\{Degree(G_j)\}}{\sum_{k=1}^{N}\{Degree(G_0)\}}, j = 1, \ldots, E; G_0 = G \tag{14}$$

to illustrate the application of disease spread probability in a complex network, we calculate the spread probability after removing 2 first top ranking nodes as follows,

$$P(G_2) = \frac{12-2+1}{12} \times \frac{\sum_{k=1}^{12}\{2,1,1,4,3,3,4,1,1,1\}}{\sum_{k=1}^{12}\{2,1,4,3,3,3,5,1,1,1,1,1\}} = \frac{11}{12} \times \frac{21}{26} = \mathbf{0.7404}.$$

therefore, the pandemic disease spread probability in the complex network containing 12 nodes and 13 edges (see Fig. 1) with deleting the 2 first top-ranking nodes, will decrease $P(G_0) - P(G_2) = 1 - 0.7404 = 0.2596$.

Figs. 5–8 illustrate the decreasing of pandemic disease spread probabilities for the graphs 1–4 shown in the Figs. 1–4, by removing step-by-step nine infected top-ranking nodes. It can be seen that by removing the first few influential nodes with top ranking, the probability of spreading the pandemic disease decreases more rapidly. It is assumed that disease spread probability is equal 1, for the proposed graph network without removing of any node. The results show the power of effective nodes in spreading pandemic disease in a complex network. Therefore, influential nodes quarantine can be very effective in controlling the spread of pandemic diseases, including COVID-19.

2.6. Node ranking performance evaluation with SIR model

The SIR (Susceptible–Infected-Recovered) model [37,38] has been applied for the evaluation of node ranking performance [39]. The spread power of top-ranked nodes can be evaluated using SIR model. Fig. 9 shows an SIR model for epidemic disease transmission in a population of high-risk individuals.

The dynamic system of SIR model can be mathematically shown as follows,

$$\begin{cases} \frac{dS}{dt} = -\lambda S, \\ \frac{dI}{dt} = \lambda S - \gamma I, \\ \frac{dR}{dt} = \gamma I, \end{cases} \tag{15}$$

where, γ is the rate of recovered people from the infected people, λ is the infection rate and depends on the transmission probability per partner ($\beta > 0$), the number of partners per individual per unit time ($r > 0$), and the proportion of infected individuals to sexually active individuals $\frac{I}{I+S+R}$ as follows,

$$\lambda = r\beta \frac{I}{S+I+R}.$$

Table 1
Decision matrix $D = (x_{ij})$.

Degrees centrality	Betweenness centrality	Eigenvector centrality
2	68	0.2866
1	60	0.1316
1	39	0.1316
4	39	0.3622
3	**13**	**0.4468**
3	3	0.4267
3	0	0.4408
5	0	0.3394
1	0	0.1233
1	0	0.1233
1	0	0.1233
1	0	0.1233

Table 2
Nodes ranking based on relative closeness to the ideal solution for the graph showed in the Fig. 1 [34].

Nodes	S_i^+	S_i^-	C_i	Ranking
1	0.1935	0.0508	0.2080	8
2	0.2226	0.0623	0.2187	7
3	0.2226	0.0623	0.2187	6
4	0.0868	0.1506	0.6344	2
5	**0.1170**	**0.1199**	**0.5062**	**4**
6	0.1564	0.0860	0.3547	5
7	0.1024	0.1592	0.6086	3
8	0.0545	0.2227	0.8034	1
9	0.2231	0.0467	0.1732	12
10	0.2231	0.0467	0.1732	11
11	0.2231	0.0467	0.1732	10
12	0.2231	0.0467	0.1732	9

Table 3
Nodes ranking based on relative closeness to the ideal solution for the graph showed in the Fig. 2 [35].

Nodes	S_i^+	S_i^-	C_i	Ranking
1	0.2155	0.0686	0.2414	9
2	0.2177	0.0444	0.1693	13
3	0.1280	0.1078	0.4572	4
4	0.0766	0.2153	0.7375	1
5	0.1672	0.0935	0.3587	6
6	0.1807	0.0702	0.2798	7
7	0.2177	0.0444	0.1693	12
8	0.1457	0.0986	0.4036	5
9	0.0789	0.1898	0.7062	2
10	0.1990	0.0503	0.2017	11
11	0.1990	0.0503	0.2017	10
12	0.1268	0.1088	0.4619	2
13	0.2153	0.0766	0.2625	8

In the proposed model, the susceptible population or healthy nodes in class S will be infected with the transmission rate λ. Using the initial conditions $S(0) = S_0$, $I(0) = I_0$ and $R(0) = R_0$ analytical solutions of systems (15) are as follows,

$$\begin{cases} S(t) = S_0 e^{-\overline{\lambda}t}, \\ I(t) = \dfrac{\left(\overline{\lambda} S_0 e^{(\gamma-\overline{\lambda})t} - (S_0 + I_0)\overline{\lambda} + \gamma I_0\right) e^{-\gamma t}}{\gamma - \overline{\lambda}}, \\ R(t) = S_0 + I_0 + R_0 + \dfrac{((S_0 + I_0)\overline{\lambda} - \gamma I_0) e^{-\gamma t} - \gamma S_0 e^{-\overline{\lambda}t}}{\gamma - \overline{\lambda}}, \end{cases} \tag{16}$$

In the SIR model, $S(t)$ represents the number of susceptible nodes or healthy individuals, $I(t)$ denotes the number of infected nodes or infected individuals that are capable to propagate the disease to healthy individuals or susceptible individuals, and $R(t)$ is the recovered people from infected people. One randomly susceptible neighbor gets infected by each infected node with the probability of λ at each step. In this paper, infection rate was assumed to be $\lambda = \overline{\lambda} = 0.3$ and recovered ratio was assumed to be $\gamma = 0.05$ for uniformity purposes. Transmission rate can specify the influence range of a node in the epidemic spread on networks. Disease can spread to its higher order neighbors through the intermediaries not only to its immediate neighbors by an infected node. Therefore, detection of the influential nodes plays an important role in the spread of an epidemic disease on networks.

Table 4
Nodes ranking based on relative closeness to the ideal solution for the graph showed in the Fig. 3 [1].

Nodes	S_i^+	S_i^-	C_i	Ranking
1	0.0253	0.1924	0.8836	1
2	0.1759	0.0412	0.1899	22
3	0.1606	0.0547	0.2540	16
4	0.1759	0.0412	0.1899	21
5	0.1919	0.0364	0.1593	23
6	0.1326	0.1137	0.4616	4
7	0.1759	0.0412	0.1899	20
8	0.1606	0.0547	0.2540	15
9	0.1759	0.0412	0.1899	19
10	0.1136	0.1240	0.5221	3
11	0.1171	0.0807	0.4078	5
12	0.1393	0.0669	0.3246	11
13	0.1464	0.0697	0.3226	12
14	0.1403	0.0667	0.3222	13
15	0.1427	0.0688	0.3254	10
16	0.1367	0.0694	0.3366	8
17	0.1408	0.0691	0.3293	9
18	0.1585	0.0576	0.2666	14
19	0.1570	0.0517	0.2479	17
20	0.1339	0.0685	0.3385	7
21	0.1340	0.0686	0.3388	6
22	0.1489	0.0489	0.2472	18
23	0.0859	0.1157	0.5737	2

Table 5
Nodes ranking based on relative closeness to the ideal solution for the graph showed in the Fig. 4 [36].

Nodes	S_i^+	S_i^-	C_i	Ranking
1	0.0696	0.2066	0.7479	1
2	0.1545	0.0649	0.2957	9
3	0.1545	0.0649	0.2957	8
4	0.1273	0.1267	0.4990	2
5	0.2124	0.0220	0.0938	23
6	0.2124	0.0220	0.0938	22
7	0.2124	0.0220	0.0938	21
8	0.2124	0.0220	0.0938	20
9	0.2092	0.0385	0.1554	18
10	0.2092	0.0385	0.1554	17
11	0.2092	0.0385	0.1554	16
12	0.2092	0.0385	0.1554	15
13	0.1164	0.1090	0.4837	13
14	0.1635	0.0585	0.2637	10
15	0.1711	0.0569	0.2495	13
16	0.1435	0.0844	0.3704	7
17	0.1393	0.0865	0.3832	6
18	0.1335	0.0911	0.4057	5
19	0.1909	0.0463	0.1953	14
20	0.1766	0.0601	0.2540	12
21	0.2098	0.0348	0.1424	19
22	0.2128	0.0202	0.0865	24
23	0.1280	0.1188	0.4814	4
24	0.2066	0.0715	0.2571	11

3. Results and discussion

This Section study about two network graphs for the pandemic COVID-19 from references [85, 86]. Fig. 10 shows the flow chart of the proposed method. First graph shows six regions of Portugal and some of their connections [40]. Three top ranking nodes for this graph are highlighted with the red color (Fig. 11). Second graph presents Greek COVID-19 infection visibility [41]. Nine top ranking nodes are highlighted with red color (Fig. 12). According to Fig. 11, the regions Centro, Lisboa e Vale do Tejo and Alentejo are influential

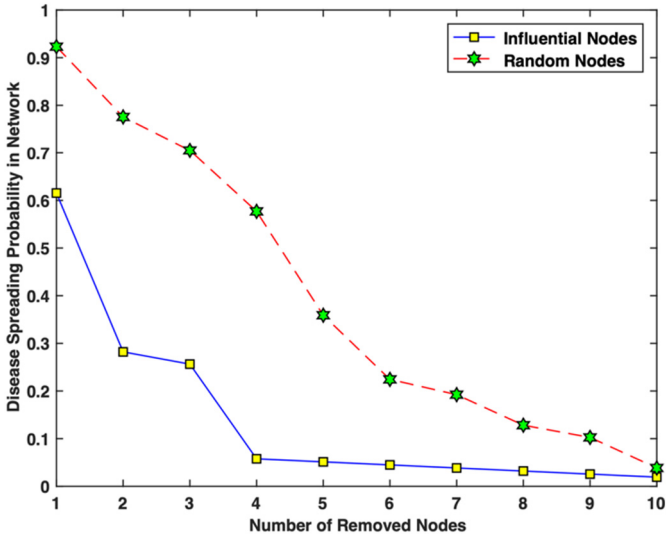

Fig. 5. Probability of disease spreading for graph 1.

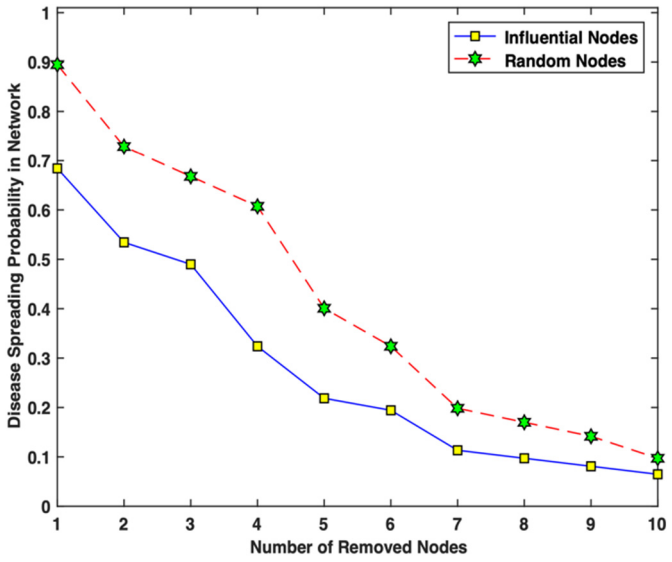

Fig. 6. Probability of disease spreading in graph 2.

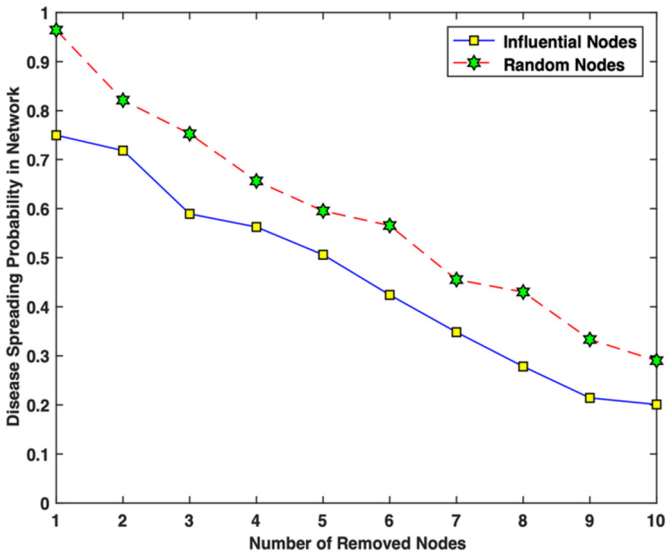

Fig. 8. Probability of disease spreading for graph 4.

areas. Quarantine each of these areas will decrease the outbreak of pandemic COVID-19, and probability of pandemic disease spread decreases more rapidly.

In this paper, many of centrality measures and their applications were used for detecting influential nodes. All those methods have some restrictions and drawbacks and all have only focused on one centrality measure. The information flows are pivotal to identify the influential nodes in a network. As pointed by several authors, it is necessary to employ different types of centrality measures in different networks with different information [12,14–16].

3.1. Analysis of Portugal regions

Fig. 11 shows Portugal's graph of six regions: *(1) Norte; (2) Centro; (3) Lisboa e Vale do Tejo; (4) Alentejo; (5) Algarve; (6) Pinhal Litoral* [40]. The graph consists of 6 nodes and 7 edges and three top-ranking nodes are highlighted with the red color. Table 6 highlights the top ranked nodes by DC measure, CC measure, BC measure, EC measure, basic TOPSIS method and proposed method for the network of six Portugal regions. Table 3 shows that we get same results for the proposed method, basic TOPSIS method and BC measure method. The disease spreading probability for Portugal's six regions has been illustrated in Fig. 11. It can be seen from Fig. 12, if the three effective nodes are removed, the probability of COVID-19 transmission decreases more rapidly (decreases from $P(G_0) = 1$ to $P(G_3) = 0.2562$).

Fig. 13. shows the infected cumulative number versus time between node 4 and node 2 for the six regions network of Portugal. According to the Fig. 13, node 4 infects the entire network nodes more quickly, so node 4 ranks higher than node 2. Therefore, the proposed method works better than the DC method. The number of cumulative infected cases versus time between node 4 and node 5 for the above network is shown in the Fig. 14. According to the analysis, node 4 performs better than node 5 in terms of infecting all network nodes. Hence, the proposed method works better than the CC and EC methods. Table 6 summarizes the order of running time using the DC measure, CC measure, BC measure, EC measure, basic TOPSIS method and proposed method for the six Portugal regions network is as $RT_{DC} < RT_{EC} < RT_{BC} < RT_{CC} < RT_{TOPSIS\ METHOD} < RT_{PROPOSED\ METHOD}$ (RT: Running Time).

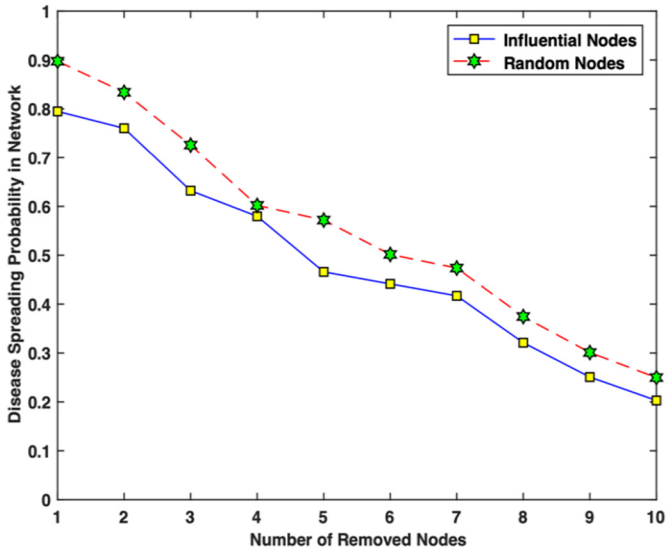

Fig. 7. Probability of disease spreading for graph 3.

3.2. Analysis of Greece

Fig. 15 illustrates the network overview of Greek's COVID-19 transmission [41]. The network graph consists of 43 nodes and 107 edges and nine top ranking nodes are highlighted with the red color. As shown in the Fig. 15, the proposed network graph is divided into five clusters namely Q_1 to Q_5. Out of the top nine nodes, four nodes as 9, 11, 17 and 19 with rank of 5, 8, 3 and 1 respectively, are ranked in the first cluster Q_1. None of the nine effective nodes are located in the second cluster Q_2. Influential nodes 26 and 32 with rank of 5 and 7 are

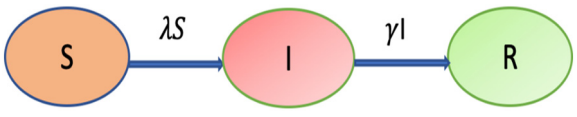

Fig. 9. A schematic of SIR model.

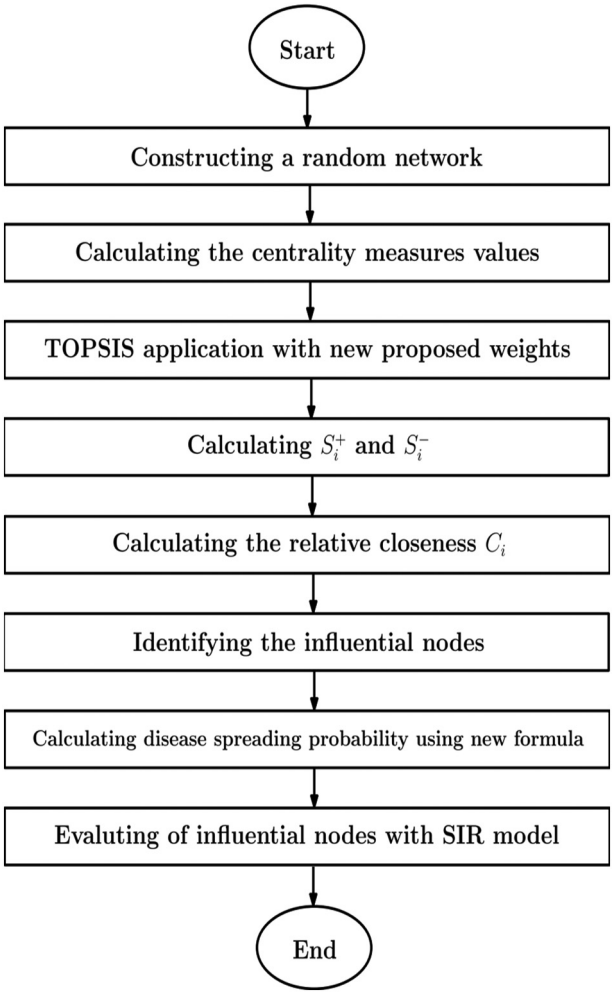

Fig. 10. Flow chart of proposed method.

located in the third and fourth clusters Q_3 and Q_4 respectively, whereas three nodes 35, 37 and 42 with rank of 4, 2 and 9 respectively belong to the fifth cluster Q_5.

Table 7 presents the summary of the top nine ranked nodes by DC measure, BC measure, EC measure, basic TOPSIS method and proposed method for the Greek COVID-19 infection visibility network [41]. The order of running time using the DC measure, CC measure, BC measure, EC measure, basic TOPSIS method and proposed method for the nine Greek COVID-19 transmission network is as $RT_{BC} < RT_{EC} < RT_{DC} < RT_{CC}$

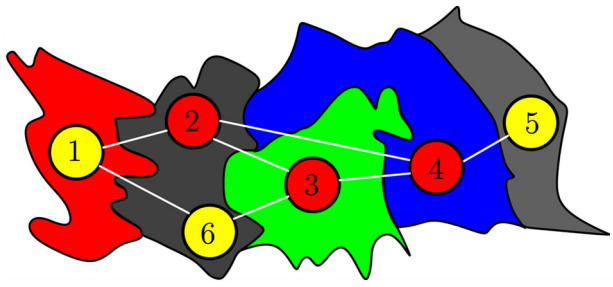

Fig. 11. Six regions of Portugal and some of their connections: *(1) Norte; (2) Centro; (3) Lisboa e Vale do Tejo; (4) Alentejo; (5) Algarve; (6) Pinhal Litoral* [40]. Three top ranking nodes highlighted with red color.

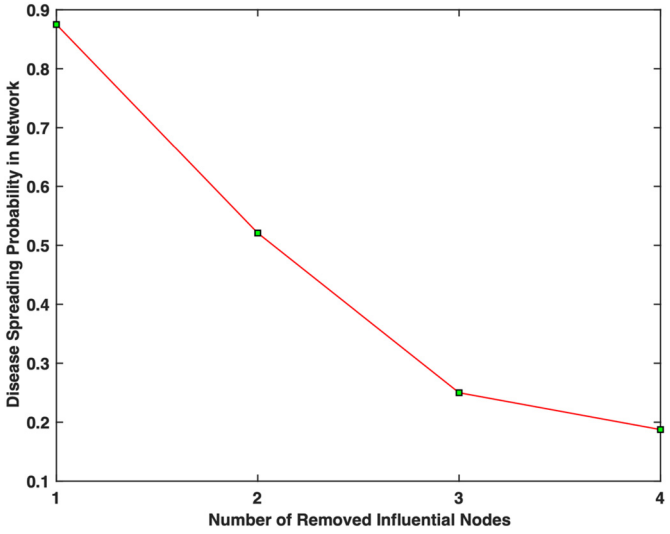

Fig. 12. Probability of disease spreading in the network of six regions of Portugal [40].

$< RT_{TOPSIS\ METHOD} < RT_{PROPOSED\ METHOD}$ (RT: Running Time). The disease spreading probability for the Greek COVID-19 infection visibility network with removal of nine influential nodes is shown in the Fig. 16. It can be seen from Fig. 16, the transmission probability of COVID-19 decreases more rapidly (decreases from $P(G_0) = 1$ to $P(G_3) = 0.8137$) as the five effective nodes are removed.

Fig. 17 shows the infected cumulative number versus time graph between node 19 and node 37 for the Greek's network. It highlights the fact that node 19 infects all healthy nodes of network faster than node 37, hence node 19 ranks higher than node 37 in terms of ranking. Infected cumulative number versus time between node 9 and node 32 for the Greek Covid-19 infection network is presented in the Fig. 18. From the results we have found that node 9 can infect all healthy nodes of network faster than node 32, therefore node 9 ranks higher than node 37 in terms of ranking.

Fig. 19 shows the infected cumulative number versus the time graph between node 42 and node 23 for the Greek's network. As can be seen, node 42 infects all network healthy nodes much faster than node 23, so node 42 ranks higher than node 23. Infected cumulative number versus time between node 37 and node 17 for the Greek's network is illustrated in Fig. 20. Results depict that node 37 and node 17 can infect all healthy nodes of the network with almost the same speed and power. It can be seen that between times 1 to 9, node 17 works better than node 37, but between times 9 to 21, opposite phenomenon is evident. Fig. 21 shows the number of cumulative cases versus the time between node 19 and node 43 for the Greek's network. It is also evident that node 19 infects all network healthy nodes much faster than node 43.

Table 6
The top six ranked nodes by DC measure, CC measure, BC measure, EC measure, basic TOPSIS method and proposed method for the network of six Portugal regions [40].

Rank	DC	CC	BC	EC	Basic TOPSIS method	Proposed method
1	2	5	4	5	4	4
2	6	1	2	1	2	2
3	4	6	3	4	3	3
4	3	4	6	6	6	6
5	1	3	5	3	5	5
6	5	2	1	2	1	1
Running time (s)	0.0448	0.0496	0.0462	0.0452	0.3262	0.3349

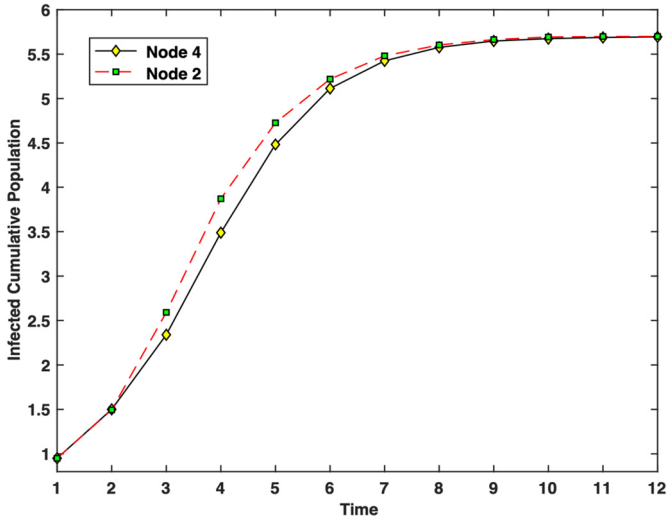

Fig. 13. Infected cumulative number versus time between node 4 and node 2 for the Portugal six regions network.

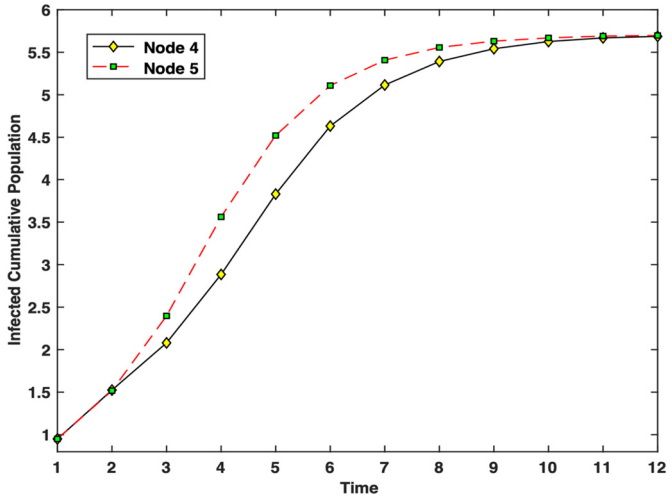

Fig. 14. Infected cumulative number versus time between node 4 and node 5 for the Portugal six regions network.

Table 7
The top nine ranked nodes by DC measure, BC measure, EC measure, basic TOPSIS method and proposed method in the network of Greek Covid-19 infection visibility [41].

Rank	DC	CC	BC	EC	Basic TOPSIS method	Proposed method
1	19	43	19	43	19	19
2	17	28	37	28	37	37
3	37	42	35	27	17	17
4	9	31	32	31	35	35
5	35	27	17	29	32	9
6	26	29	26	42	9	26
7	11	7	9	38	26	32
8	32	8	42	41	11	11
9	23	14	11	39	42	42
Running time (s)	0.0493	0.2043	0.0479	0.0483	2.4996	2.5622

4. Conclusion

To detect the influential nodes with high accuracy in a complex social network, a modified TOPSIS method has been proposed to obtain more efficient weights. This study shows how to detect influential nodes in a complex network more effectively in controlling COVID-19 transmission in a population. The spreading probabilities of influential nodes have also been calculated using a novel proposed formula, which also illustrate the rank wise importance of key nodes. Experimental results highlight that removal of the influential nodes can decrease the transmission probability of COVID-19. Therefore, detection of influential nodes in a COVID-19 complex network could be really insightful in terms of slowing down the rate of disease transmission. The SIR epidemic model was used in two real COVID-19 transmission networks to verify the efficiency of the proposed method. The results show that the proposed method is more successful in finding effective nodes with higher accuracy than traditional methods.

CRediT authorship contribution statement

All authors have contributed equally to produce this study.

Declaration of competing interest

The author(s) declared no potential conflicts of interest with respect to the research, authorship, and/or publication of this article.

Acknowledgment

The authors are pleased to acknowledge the support of the National Sciences and Engineering Research Council of Canada.

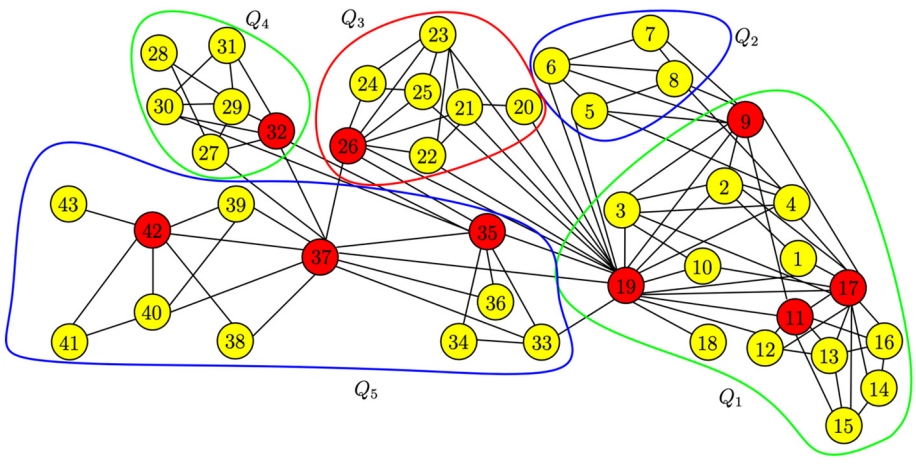

Fig. 15. Greek's COVID-19 infection visibility [41]. Nine top ranking nodes highlighted with red color.

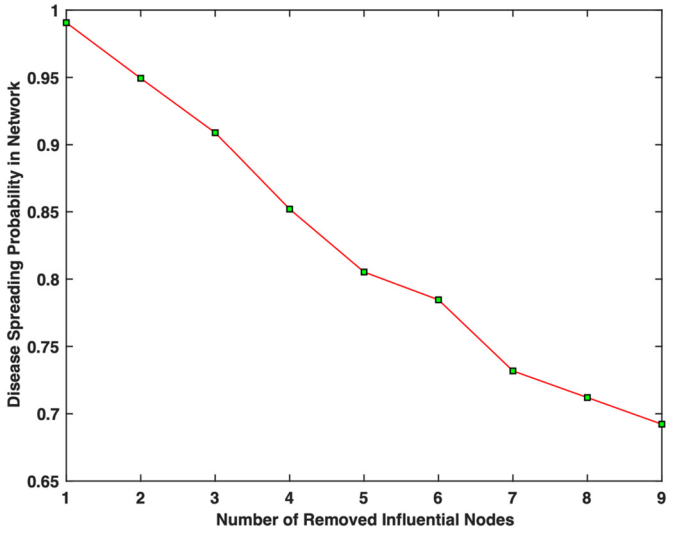

Fig. 16. Probability of disease spreading in the network of Greek's COVID-19 infection visibility [41].

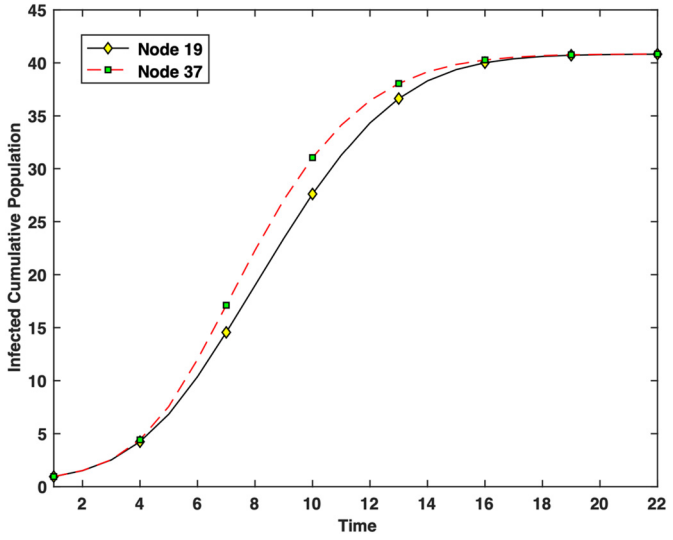

Fig. 17. Infected cumulative number versus time between node 19 and node 37 in the network of Greek [41].

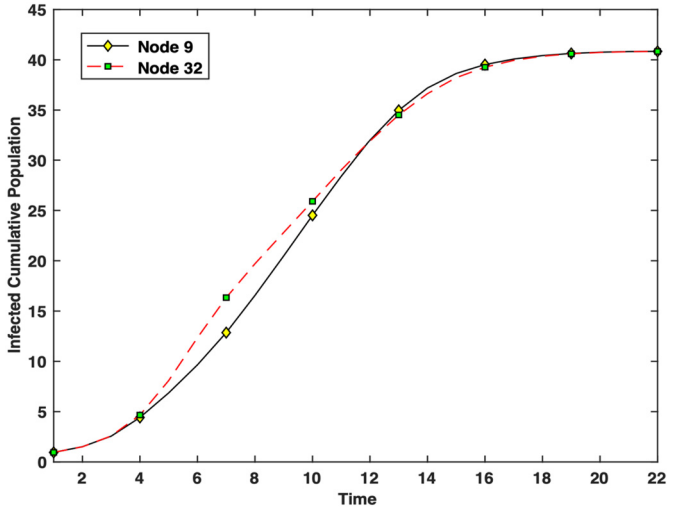

Fig. 18. Infected cumulative number versus time between node 9 and node 32 in the network of Greek [41].

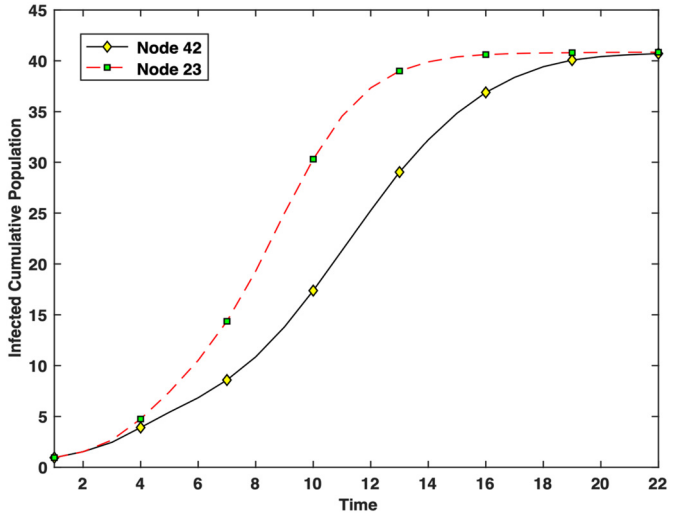

Fig. 19. Infected cumulative number versus time between node 42 and node 23 in the network of Greek [41].

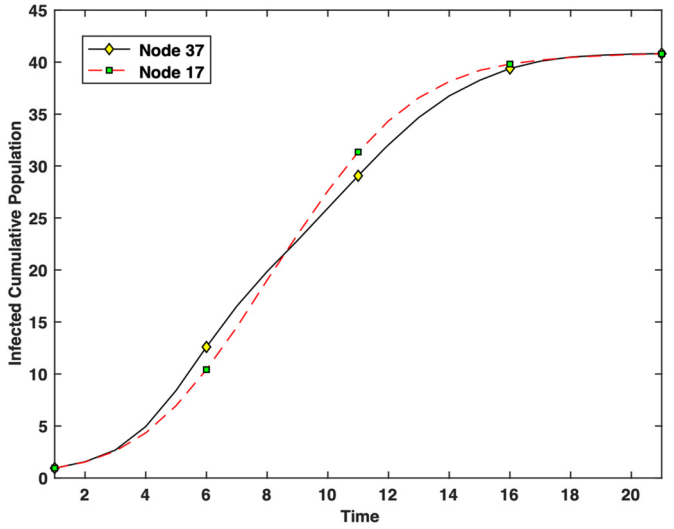

Fig. 20. Infected cumulative number versus time between node 37 and node 17 in the network of Greek [41].

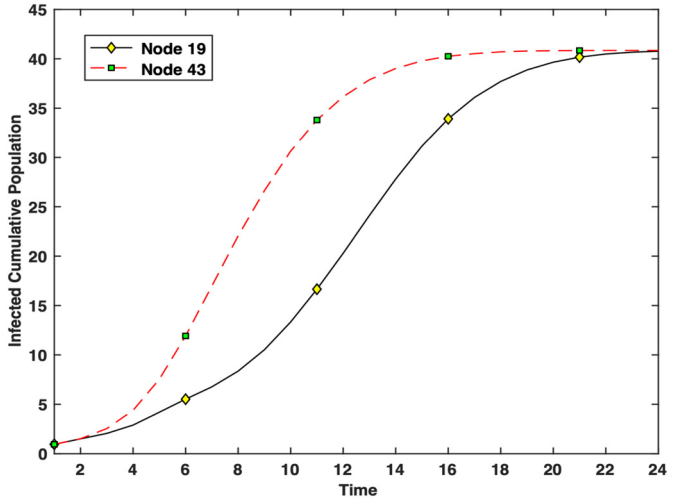

Fig. 21. Infected cumulative number versus time between node 19 and node 43 in the network of Greek [41].

References

[1] Chen D, Lü L, Shang MS, Zhang YC, Zhou T. Identifying influential nodes in complex networks. Physica A. 2012;391(4):1777–87.
[2] Zhang X, Zhu J, Wang Q, Zhao H. Identifying influential nodes in complex networks with community structure. Knowl-Based Syst. 2013;42:74–84.
[3] Du Y, Gao C, Hu Y, Mahadevan S, Deng Y. A new method of identifying influential nodes in complex networks based on TOPSIS. Physica A. 2014;399:57–69.
[4] Malliaros FD, Rossi MEG, Vazirgiannis M. Locating influential nodes in complex networks. Sci Rep. 2016;6(1):1–10.
[5] Bian T, Deng Y. Identifying influential nodes in complex networks: a node information dimension approach. Chaos. 2018;28(4):043109.
[6] Namtirtha A, Dutta A, Dutta B, Sundararajan A, Simmhan Y. Best influential spreaders identification using network global structural properties. Sci Rep. 2021; 11(1):1–15.
[7] Salavati C, Abdollahpouri A, Manbari Z. Ranking nodes in complex networks based on local structure and improving closeness centrality. Neurocomputing. 2019;336: 36–45.
[8] Liao H, et al. Ranking in evolving complex networks. Phys Rep. 2017;689:1–54.
[9] Iannelli F, et al. Influencers identification in complex networks through reaction-diffusion dynamics. Phys Rev E. 2018;98(6):15.
[10] Zareie A, et al. Influence maximization in social networks based on TOPSIS. Expert Syst Appl. 2018;108:96–107.
[11] Sheikhahmadi A, et al. Identification of influential users by neighbors in online social networks. Physica A. 2017;486:517–34.
[12] Mojzisch A, Frisch JU, Doehne M, Reder M, Häusser JA. Interactive effects of social network centrality and social identification on stress. Br J Psychol. 2020;112:144–62.
[13] Paidar M, Chaharborj SS, Harounabadi A. Identifying top-k Most influential nodes by using the topological diffusion models in the complex networks. Network. 2017.;4 (5).
[14] O. Ledesma González R. Merinero-Rodríguez J. I. Pulido-Fernández Tourist destination development and social network analysis: what does degree centrality contribute? Int J Tour Res.
[15] Das K, Mahapatra R, Samanta S, Pal A. Influential nodes in social networks: centrality measures. Handbook of research on advanced applications of graph theory in modern society. IGI Global; 2020. p. 371–85.
[16] De SS, Dehuri S, Cho SB. Research contributions published on betweenness centrality algorithm: modelling to analysis in the context of social networking. Int J Soc Netw Min. 2020;3(1):1–34.
[17] Bonacich P. Factoring and weighting approaches to status scores and clique identification. J Math Sociol. 1972;2(1):113–20.
[18] Bellingeri M, Bevacqua D, Scotognella F, Alfieri R, Nguyen Q, Montepietra D, Cassi D. Link and node removal in real social networks: a review; 2020.
[19] Çelikbilek Y, Tüysüz F. An in-depth review of theory of the TOPSIS method: an experimental analysis. J Manag Anal. 2020;7(2):281–300.
[20] Hwang CL, Yoon K. Methods for multiple attribute decision making. Multiple attribute decision making. Berlin, Heidelberg: Springer; 1981. p. 58–191.
[21] Ye Y. Passive network evolution promotes group welfare in complex networks. Chaos Solitons Fractals. 2020;130:109464.
[22] Liu F, et al. GMM: a generalized mechanics model for identifying the importance of nodes in complex networks. Knowl-Based Syst. 2020;193:105464.
[23] Wen T, et al. Vital spreaders identification in complex networks with multi-local dimension. Knowl-Based Syst. 2020;195:105717.
[24] Zhao J, Deng Y. Complex network modeling of evidence theory. IEEE Trans Fuzzy Syst. 2021;29(11):3470–80.
[25] Zhao J, et al. The identification of influential nodes based on structure similarity. Connect Sci. 2021;33(2):201–18.
[26] Yu E, Fu Y, Tang Q, Zhao JY, Chen DB. A re-ranking algorithm for identifying influential nodes in complex networks. IEEE Access. 2020;8:211281–90.
[27] Yang XH, Xiong Z, Ma F, Chen X, Ruan Z, Jiang P, Xu X. Identifying influential spreaders in complex networks based on network embedding and node local centrality. Physica A. 2021;573:125971.
[28] Li H, Shang Q, Deng Y. A generalized gravity model for influential spreaders identification in complex networks. Chaos Solitons Fractals. 2021;143:110456.
[29] Gupta M, Mishra R. Spreading the information in complex networks: identifying a set of top-N influential nodes using network structure. Decis Support Syst. 2021.; 113608.
[30] Nabi KN. Forecasting COVID-19 pandemic: a data-driven analysis. Chaos Solitons Fractals. 2020;139:110046.
[31] Nabi KN, Abboubakar H, Kumar P. Forecasting of COVID-19 pandemic: from integer derivatives to fractional derivatives. Chaos Solitons Fractals. 2020;141:110283.
[32] Nabi KN, Kumar P, Erturk VS. Projections and fractional dynamics of COVID-19 with optimal control strategies. Chaos Solitons Fractals. 2021;145:110689.
[33] Nabi KN. Epidemic prediction and analysis of COVID-19: a mathematical modelling study. In: Azar AT, Hassanien AE, editors. Modeling, control and drug development for COVID-19 outbreak prevention. Studies in systems, decision and control. Cham: Springer; 2022.
[34] Sheng J, Dai J, Wang B, Duan G, Long J, Zhang J, Guan W. Identifying influential nodes in complex networks based on global and local structure. Physica A. 2020; 541:123262.
[35] Zhu J, Wang L. Identifying influential nodes in complex networks based on node itself and neighbor layer information. Symmetry. 2021;13(9):1570.
[36] Shao Z, Liu S, Zhao Y, Liu Y. Identifying influential nodes in complex networks based on neighbours and edges. Peer-to-Peer Netw Appl. 2019;12(6):1528–37.
[37] Chaharborj SS, Fudziah I, Bakar MA, Chaharborj RS, Majid ZA, Ahmad AGB. The use of generation stochastic models to study an epidemic disease. Adv Difference Equ. 2013;2013(1):7.
[38] Kudryashov NA, Chmykhov MA, Vigdorowitsch M. Analytical features of the SIR model and their applications to COVID-19. Appl Math Model. 2021;90:466–73.
[39] Du Y, Gao C, Hu Y, Mahadevan S, Deng Y. A new method of identifying influential nodes in complex networks based on TOPSIS. Physica A. 2014;399:57–69.
[40] Silva CJ, Cantin G, Cruz C, Fonseca-Pinto R, Passadouro R, Dos Santos ES, Torres DF. Complex network model for COVID-19: human behavior, pseudo-periodic solutions and multiple epidemic waves. J Math Anal Appl. 2021.;125171.
[41] Demertzis K, Tsiotas D, Magafas L. Modeling and forecasting the COVID-19 temporal spread in Greece: an exploratory approach based on complex network defined splines. Int J Environ Res Public Health. 2020;17(13):4693.
[42] Ovi MA, Nabi KN, Kabir KMA. Social distancing as a public-good dilemma for socio-economic cost: an evolutionary game approach. Chaos Solitons Fractals. 2022.;159.